

# Elucidating the Mechanism of Shock Wave Generation within a Subsonic Reaction Wave through Extension of Zel'dovich's Ignition Front Theory

Haru Okada<sup>1,2</sup>, Youhi Morii<sup>1</sup>, Akira Tsunoda<sup>1,2</sup>, Kaoru Maruta<sup>1</sup>  
Institute of Fluid Science, Tohoku University, Sendai, Miyagi, Japan  
School of Engineering, Tohoku University, Sendai, Miyagi, Japan

## 1 Introduction

Deflagration to Detonation Transition (DDT) is a phenomenon where a flame transitions into a detonation, involving a complex interplay of flames, shock waves, turbulence, boundary layers, and localized ignition events (hot spot)[1,2]. DDT is essential for preventing explosion accidents and developing efficient combustors. Gu et al. [3] performed numerical simulations and successfully explained the DDT mechanism triggered by a hot spot using the concept of Zel'dovich's ignition front speed ( $u_{sp}$ ), defined by the spatial gradient of the ignition delay time ( $\tau_{ig}$ ), and the existence of a reaction wave propagating at the speed of  $u_{sp}$ [4]. According to Zel'dovich's theory, by comparing characteristic propagating speeds, the modes of reaction waves are classified into the following four classifications. (1)  $u_{sp} \leq S_L$  : laminar flame, (2)  $S_L < u_{sp} < a$  : Zel'dovich's ignition front, (3)  $a \leq u_{sp} \leq D_{CJ}$  : detonation, (4)  $D_{CJ} < u_{sp}$  : weak detonation, where  $S_L$  is the laminar flame speed,  $a$  is the sound speed and  $D_{CJ}$  is the CJ (Chapman-Jouguet) speed.

However, Liberman et al. [5] have reported a DDT in which the detonation originates from within a laminar flame structure. Their observations reveal that the temperature of the compressed mixture near the flame does not exceed 850 K, ruling out the conventional Zel'dovich gradient mechanism. Consequently, these findings necessitate the incorporation of additional theoretical perspectives to fully elucidate the underlying mechanisms responsible for this phenomenon. In the present paper, we show that by extending the conventional Zel'dovich gradient mechanism to the inside of laminar flame structures, the DDT onset from laminar flames can be explained within the framework of Zel'dovich gradient mechanism. Although turbulence and boundary layer effects play significant roles in DDT, our study focuses on a key element of the Zel'dovich gradient mechanism—the interplay between chemical reactions and sound speed. To eliminate extraneous complexity, we employ a one-dimensional system based on Morii et al. [6]. They conducted numerical experiments on a one-dimensional system in which high-temperature premixed gas flows into the system from the inlet boundary at a specific inlet flow velocity ( $u_{in}$ ), burns in the system, and then flows out from the outlet boundary as burnt gas to investigate the relationship between ignition, flame, and detonation. This system assumes a standing detonation engine, which is a steady propagation of detonation within the system. The results show the existence of new propagation modes governed by autoignition reaction, distinct from flame and

detonation. The reaction waves appears in the case of  $u_{\text{in}} > S_L$  or  $u_{\text{in}} > D_{\text{CJ}}$ , and the new reaction waves are formed at the position ( $x_{\text{ig}} = u_{\text{in}}\tau_{\text{ref}} = u_{\text{in}}\tau_{\text{ig}}$ ) where the residence time of the mixture ( $\tau_{\text{ref}} = \int_0^x u^{-1}(s) ds$ ) matches the ignition delay time ( $\tau_{\text{ig}}$ ) of the inflow mixture. Therefore, this reaction wave propagates autonomously due to autoignition. Morii et al. termed this reaction wave as an *autoignitive reaction wave*. From the definition of the autoignitive reaction waves, its position  $x_{\text{ig}}$  is determined by  $\tau_{\text{ig}}$ , independent of  $S_L$  and  $D_{\text{CJ}}$ . Furthermore, it was confirmed that the autoignitive reaction wave transitions to detonation when the inflow velocity is slightly less than  $D_{\text{CJ}}$ , but the principle and detailed inlet velocity conditions of DDT have not been studied and are not yet understood.

Although multidimensional approaches dominate DDT research, we believe that returning to the fundamentals by employing a simple one-dimensional system to identify the key elements of the phenomenon is both insightful and meaningful. Therefore, the purpose of this study is to investigate the autoignitive reaction wave using the same one-dimensional system with the previous papers [6, 7], to clarify the boundary conditions under which DDT occurs, and to clarify what physical phenomena govern that boundary.

## 2 Numerical methods and conditions

The compressible Navier-Stokes equations with conservation equations for chemical species were solved using an in-house code, COGNAC [8]. A one-dimensional system in which a mixture with a high temperature flows in from the inlet boundary, ignites, and then burned gas flows out from the outlet boundary was considered following the paper by Morii et al. [6]. The pressure was set to 1.0 atm at the outlet boundary. Although the current boundary conditions employed in this study did not significantly affect the results, oscillatory behavior was observed under certain conditions. In future work, active vibration suppression techniques such as Navier Stokes Characteristic Boundary Conditions (NSCBC) [9] will be incorporated to further mitigate these oscillations. For the inlet boundary conditions, the unburned mixture was the stoichiometric methane/air gas mixture, the initial temperature was set to 1600.0 K, and the mass flow rate was fixed. The inlet mass flow rate was evaluated using the density of the stoichiometric methane/air mixture multiplied by the inlet velocity. As an initial condition, the computational domain was filled with nitrogen at the same temperature and velocity as the inlet boundary conditions. GRI Mech 3.0[10] was used as the detailed chemical reaction mechanism.

Figure 1 shows the diagram of the reaction wave modes for the reaction wave position ( $x_{\text{ig}}$ ) created by the preliminary calculations to determine the target conditions. The solid line shows the positions where autoignition reaction waves stand ( $x_{\text{ig}}$ ) defined by the product of the inlet flow velocity and ignition delay time at each inlet boundary temperature, based on the results of a 0D ignition calculation using Cantera [11]. The dashed lines with  $\circ$ ,  $\diamond$ , and  $\square$  markers indicate the laminar flame speed ( $S_L$ ) calculated by Cantera, the ‘‘Shock wave in reaction wave’’, and the CJ speed ( $D_{\text{CJ}}$ ) calculated by the Shock and Detonation Toolbox [12], respectively. ‘‘Shock wave in reaction wave’’ indicates the lowest inlet velocity of the 1D laminar flame calculation using Cantera where the local flow velocity inside of the 1D flame structure exceeds the local sound speed. This condition should be sufficient for DDT [4]. The reaction waves in the figure are divided into four regions according to the propagation modes.

1. Unsteady state solution: this is the region of a laminar flame, where the reaction wave propagates toward upstream and flashback because  $u_{\text{in}} < S_L$ .
2. Steady-state solution: the laminar flame flows toward downstream because  $u_{\text{in}} > S_L$ . However, a subsonic autoignitive reaction wave is finally stationary at  $x_{\text{ig}}$ .
3. Unsteady state solution: transition from transonic autoignitive reaction wave to detonation occurs and the detonation propagates toward upstream and flashback because  $u_{\text{in}} < D_{\text{CJ}}$ .

4. Steady-state solution:  $u_{in} > D_{CJ}$ , a region of supersonic autoignitive reaction wave, where the reaction wave is located at  $x_{ig}$ [6].

In Figure 1, the dash-dotted lines with  $\circ$  and  $\square$  correspond to the boundary between the autoignitive reaction wave and the laminar flame and detonation, respectively. However, although the dashed line ( $\diamond$ ) is sufficient conditions for the transition of autoignition to detonation, necessary and sufficient conditions for the boundary between the autoignitive reaction wave while the detonation has not been clarified yet. In this study, calculations were performed at inflow velocities of 150 m/s (Case 1) and 250 m/s (Case 2) to clarify the boundary where the DDT occur or not. 12 cm (Case 1) and 25 cm (Case 2) were chosen for the computational domain so that  $x_{ig}$  is near the center of the computational domain. DDT did not occur in Case 1, whereas it occurred in Case 2.

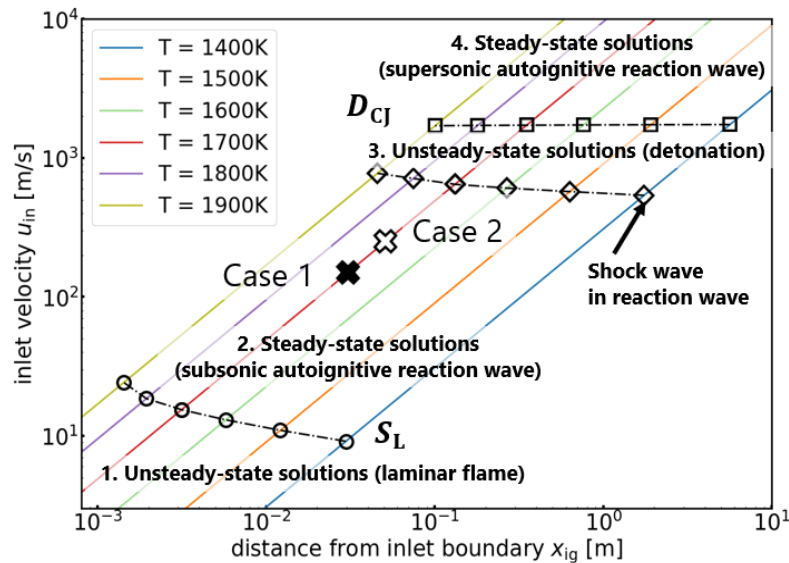


Figure 1: Reaction modes diagram for stoichiometric  $\text{CH}_4/\text{air}$  mixture at various inlet temperature conditions and the relationship of the reaction wave with respect to its position.

### 3 Results and discussion

Figure 2 (a) shows the spatial distributions of pressure and temperature at each time in Case 1. At  $t = 0 \mu\text{s}$ , the mixture starts to flow into the domain which was initially filled by nitrogen. At  $t = 500 \mu\text{s}$  in the lower part of Fig. 2 (a), a steep temperature increase appears around  $x = 7.0 \text{ cm}$ . This is because the residence time of the mixture was close to the ignition delay time, so autoignition occurred. Also, the temperature discontinuity at 5.0 cm and the corresponding pressure discontinuity at the same location appears, suggesting that these discontinuities are the weak shock generated by the autoignition. Subsequently, from  $t = 500 \mu\text{s}$  to  $t = 600 \mu\text{s}$ , the reaction wave (and the preceding weak shock) propagated toward the inlet boundary even though the inlet flow velocity was higher than the laminar flame speed (see Fig. 1). This reaction wave is not a detonation wave, as no high-pressure peak ahead of the reaction front have been observed. Therefore, this reaction wave is considered to be an autoignitive reaction wave. However, this reaction wave is not stationary at  $x_{ig}$  owing to the preceding weak shock wave ahead of the reaction wave. Specifically, the compression by the preceding weak shock could change the propagating speed of the autoignition wave estimated from the 0D ignition simulation.

Figure 2(b) shows the spatial distribution of pressure and temperature at each time in Case 2. The spatial distribution of temperature in the lower part of Fig. 2(b) shows a temperature increase due to

autoignition at  $t = 500 \mu\text{s}$  around 12 cm. After that, from  $t = 500 \mu\text{s}$  to  $t = 575 \mu\text{s}$ , the propagation of autoignition reaction wave with the preceding weak shock was observed similar to that in Case 1. From  $t = 575 \mu\text{s}$  to  $t = 620 \mu\text{s}$ , the sharp peaks of pressure and temperature gradually increase. Finally, a high-pressure peak is observed at  $t = 620 \mu\text{s}$ , which coincides with the peak position of the temperature, indicating that the reaction wave in Case 2 transition to detonation. So, the boundary of DDT is expected to exist between Case 1 and 2.

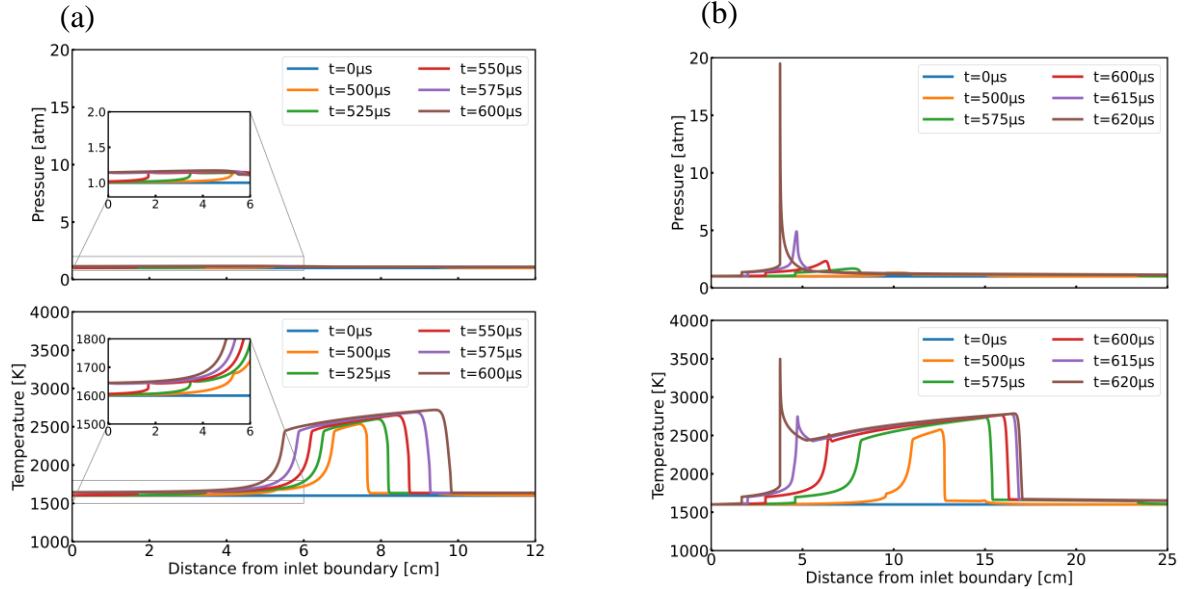


Figure 2: Temperature (bottom) and pressure (top) profiles of Case 1(a) and Case 2(b) for 500 ~ 620 $\mu\text{s}$ .

Next, we analyzed Case 1 and Case 2 using  $u_{\text{sp}}$  to find out the cause of DDT. Autoignitive reaction waves are reaction waves formed due to autoignition. In other papers [7, 13], Morii et al. proposed a theoretical consideration that the normalized reaction progress of 0D autoignition and the 1D flame structure with Lewis number 1 are equivalent. Based on this theoretical consideration, there is room to apply Zel'dovich's  $u_{\text{sp}}$  analysis, which assumes 0D autoignition at each point, to the inside of reaction wave structures such as autoignitive reaction waves. In conventional analyses,  $u_{\text{sp}}$  has been mainly used to analyze hot spots, but in this study, the concept of Zel'dovich's ignition front is extended to the inside of the reaction wave structure based on Morii's theory. As the definition of Zel'dovich's ignition front is written as  $u_{\text{sp}} = |\nabla\tau_{\text{ig}}|^{-1}$ , in this study,  $\tau_{\text{ig}}$  is calculated using the information of mixture component at each position inside the flame structure. Then,  $u_{\text{sp}}$  is derived from the spatial gradient of the ignition delay time. Two thermodynamic assumptions were used: constant enthalpy and pressure (hereafter HP) and constant internal energy and volume (hereafter UV) for the calculation of  $\tau_{\text{ig}}$  because the spontaneous reaction progress of the local mixture can be different depending on the situation. The pressure wave generated by the autoignition dissipates when the inlet velocity is slow, as it propagates forward and backward of the ignition point. When the inlet velocity is fast, however, the compression effect becomes significant, and the pressure wave generated by the autoignition gradually compresses forward of the ignition point. Therefore, under these conditions, it is thought that the premise of a UV condition is more appropriate.

In the present study,  $u_{\text{sp}}$  at the divergence of the velocity being zero is chosen as the representative, and the reason of this choice is explained as follows. In the vicinity of the reaction wave, the divergence of the flow velocity becomes positive due to the source term governed by the chemical reactions. The position where the divergence of the flow velocity becomes zero is considered to be the position where the reaction wave can influence the surroundings through exothermic reactions. Therefore, this position

is defined as the entrance of the reactive wave. The propagation velocity of the reactive wave is defined as the propagation speed of the peak of heat release rate relative to the local velocity at the position where the divergence of the velocity is zero.

Figure 3(a) shows the time histories of  $u_{sp}$  in Case 1, sound speed, and propagation velocity of the reaction wave at the position where the divergence of the flow velocity becomes zero. Only the results after  $t = 510 \mu s$ , when stable propagation of the reaction wave is confirmed after the initial disturbance, are shown. The propagation velocity of the reaction wave followed  $u_{sp}$  of the HP condition. The propagation velocity of the reaction wave was kept almost constant and did not exceed the sound speed.

The time histories of  $u_{sp}$ , sound velocity, and propagation velocity of the reaction wave in Case 2 are shown in Fig. 3(b). As in Fig. 3(a), only the results after  $t = 500 \mu s$ , when stable reaction wave propagation can be confirmed are shown. Starting from the propagation speed closer to  $u_{sp}$  of the HP condition, the propagation speed gradually approaches  $u_{sp}$  under the UV condition from  $t = 500 \mu s$  to  $t = 575 \mu s$ . The propagation speed matches  $u_{sp}$  under the UV condition at around  $t = 575 \mu s$ . The vertical dashed line indicates  $t = 575 \mu s$ , the timing at which the pressure and temperature peak values observed in Fig. 2b. Thereafter, the reaction wave propagates at the speed of  $u_{sp}$  of UV conditions. Finally,  $u_{sp}$  increases rapidly around  $t = 619 \mu s$ , exceeding the sound speed and transition to detonation.

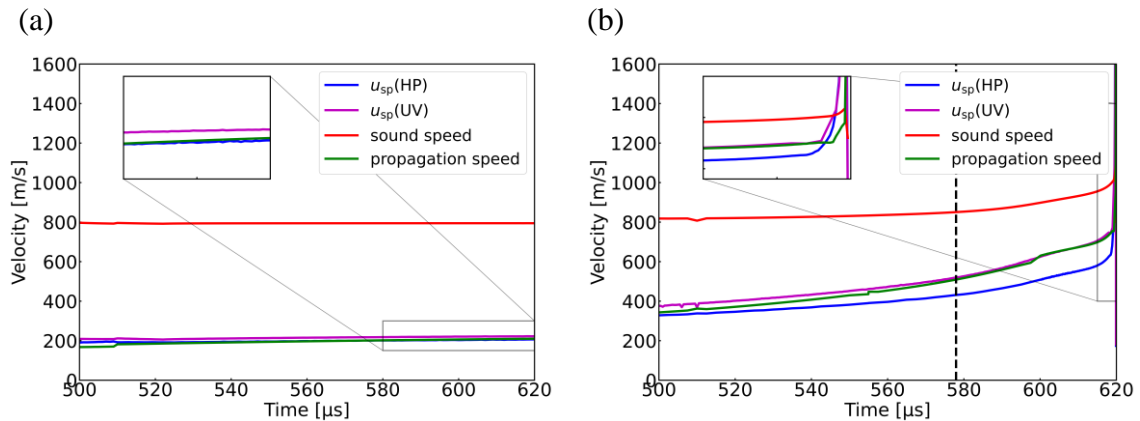


Figure 3: Time histories of  $u_{sp}$ , sound speed, and reaction wave propagation speed in Case 1 (a) and Case 2 (b).

From Fig. 3, the  $u_{sp}$  calculated for the HP and UV conditions correspond to the lower and upper limits of the propagation velocity of the autoignitive reaction wave, respectively. The propagation velocity of the autoignitive reaction wave agrees with  $u_{sp}$  calculated with either condition, except for the transition condition (Case 2,  $t = 500 \mu s$  to  $t = 575 \mu s$ ). Therefore, it is confirmed that the autoignitive reaction wave is a phenomenon equivalent to Zel'dovich's ignition front, and the definition of  $u_{sp}$  extended in the present study is valid. As observed in Fig. 3(b), the propagation velocity of the autoignitive reaction wave gradually shifts from  $u_{sp}$  of HP condition to  $u_{sp}$  of UV condition, and DDT occurs when the propagation velocity exceeds the sound speed. According to Zel'dovich's classification, Zel'dovich's ignition front propagates when  $S_L < u_{sp} < a$ , and detonation propagates when  $a \leq u_{sp} \leq D_{CJ}$ . Therefore, the extended definition also works in terms of Zel'dovich's classification. In addition, as confirmed in Fig. 3(b), the timing of shock wave formation (vertical dash line) is very close to the timing when the propagation velocity coincides with  $u_{sp}$  for UV condition, while in Fig. 3(a) the propagation velocity never approached to  $u_{sp}$  of UV condition. Once the propagation speed (under HP condition) starts approaching  $u_{sp}$  of UV condition, DDT becomes inevitable. This suggests that  $u_{sp}$  UV conditions play a critical role in DDT.

## 4 Conclusions

To clarify the detailed mechanism of DDT, numerical calculations and analyses of the behavior of reaction waves in the vicinity of DDT boundary of an autoignitive reaction wave were performed, and the following findings were obtained.

- The propagation speed of the autoignitive reaction wave coincides with Zel'dovich's ignition front speed ( $u_{sp}$ ) at the position where the divergence of the flow velocity is zero, indicating that Zel'dovich's ignition front speed concept is applicable to propagating waves.
- When  $u_{sp}$  of UV condition and propagation speed match, the reaction wave forms a shock wave that eventually transitions to detonation. In other words, it is clear that the decisive factor influencing DDT is not the relationship between  $u_{sp}$  and the sound speed, but whether the reaction wave propagates in accordance with the UV condition.
- DDT occurred when  $u_{sp}$  exceeds the sound speed.

## References

- [1] Y. Ballossier, F. Viot, and J.M. Gavilanes. (2023). Flame acceleration and detonation onset in narrow channels: Simultaneous schlieren visualization, 254: 112833
- [2] P. Urtiew, A.K. Oppenheim. (1966). Experimental observations of the transition to detonation in an explosive gas. Proc. R. Soc. London Ser. A 295: 13-28.
- [3] X.J. Gu, D.R. Emerson, and D. Bradley. (2003). Modes of reaction front propagation from hot spots. Combustion and Flame 133: 63–74.
- [4] Y. Zel'dovich. (1980). Regime classification of an exothermic reaction with nonuniform initial conditions. Combustion and Flame 39: 211–214.
- [5] M.A. Liberman, M.F. Ivanov, A.D. Kiverin, M.S. Kuznetsov, A.A. Chukalovsky, and T.V. Rakhimova. (2010). Deflagration-to-detonation transition in highly reactive combustible mixtures. Acta Astronautica 67: 688–701.
- [6] Y. Morii and K. Maruta. (2024). General concept for autoignitive reaction wave covering from subsonic to supersonic regimes. Physics of Fluids 36: 016139.
- [7] Y. Morii and K. Maruta. (2023). What connects ignition and deflagration? -- On explosive transition of deflagration. arXiv:2212.01978.
- [8] K. Akita, P. Zhao, Y. Morii, K. Maruta, D. Splitter, and F.D.F. Chuahy. (2024). Effects of unburnt reaction progress on stretch flame dynamics under elevated temperatures. Combustion and Flame 259: 113193.
- [9] T. Poinso, S. Lele. (1992). Boundary Conditions for Direct Simulations of Compressible Viscous Flows. J. Comp. Phys. 101: 104-129.
- [10] G. P. Smith, [http://www.me.berkeley.edu/gri\\_mech/](http://www.me.berkeley.edu/gri_mech/), GRI-Mech. 3.0.
- [11] D.G. Goodwin, R. L. Speth, H.K. Moffat, B.W. Weber. (2021). <https://www.cantera.org>. Version 3.0.
- [12] J.E. Shepherd. (2021). <https://shepherd.caltech.edu>. "Shock and detonation toolbox - 2021 version".
- [13] Y. Morii, A. Tsunoda, A.K. Dubey, and K. Maruta. (2023). Analysis of knock onset based on two-dimensional direct numerical simulation and theory of explosive transition of deflagration. Physics of Fluids 35: 083604.